Evaluation of Late Summer Passive Microwave Arctic Sea Ice Retrievals

Thorsten Markus and Sverre T. Dokken

Abstract—**The melt period of the Arctic sea ice cover is of particular interest in studies of climate change due to the albedo feedback mechanisms associated with meltponds and openings in the ice pack. The traditionally used satellite passive microwave sea ice concentration algorithms have deficiencies during the summer months due to the period's highly variable surface properties. A newly developed ice concentration algorithm overcomes some of these deficiencies. It corrects for low ice concentration biases caused by surface effects through the use of 85 GHz data in addition to the commonly used 19 and 37 GHz data and, thus, the definition of an additional ice type representing layering and inhomogeneities in the snow layer. This new algorithm will be the standard algorithm for Arctic sea ice concentration retrievals with the EOS Aqua advanced microwave scanning radiometer (AMSR-E) instrument. In this paper, we evaluate the performance of this algorithm for the summer period of 1996 using data from the special sensor microwave imager (SSM/I) which has frequencies similar to the AMSR instrument. The temporal evolution of summertime passive microwave sea ice signatures are investigated and sea ice concentration retrievals from the standard NASA team and the new algorithm are compared. The results show that the introduction of the additional sea ice type in the new algorithm leads to improved summertime sea ice concentrations. The SSM/I sea ice retrievals are validated using SAR-derived ice concentrations that have been convolved with the SSM/I antenna pattern to ensure an appropriate comparison. For the marginal ice zone, with ice concentrations ranging from 40% to 100%, the correlation coefficient of SAR and SSM/I retrievals is 0.66 with a bias of 5% toward higher SAR ice concentrations. For the central Arctic, where ice concentrations varied between 60% and 100%, the correlation coefficient is 0.87 with a negligible bias.**

Index Terms—**Arctic, passive microwave remote sensing, sea ice.**

I. INTRODUCTION

DURING spring and summer, the surface of the Arctic sea ice cover undergoes rapid changes that affect the surface albedo and impact the further decay of the sea ice. Later in the summer, the remaining sea ice cover sets the stage for next winter's sea ice growth. Satellite passive microwave data have widely been used to continuously monitor polar sea ice conditions. Unfortunately, summertime is the most difficult season for using passive microwave sensors to estimate accurately sea ice concentrations, i.e., the areal fraction of sea ice within a satellite pixel. The reason for this is that summer sea ice/snow surface conditions are extremely variable in time as well as in space. After the air temperatures reach 0 °C, the snow layer becomes wet, then melts and forms meltponds. These meltponds eventually melt through the sea ice causing a drainage of the pond and/or a flooding of the floes with sea water. Initially a wet snow surface behaves radiometrically as a blackbody resulting generally in overestimates of ice concentration, whereas meltponds appear as open water in the microwave signal causing an underestimate. To increase the complexity further, melt and freeze events frequently intersperse when the air temperature is oscillating about the freezing point. The evolution of summer time passive microwave signatures has been studied by several authors [1], [4], [7]– [9], [11], [14], [15], [19], [20].

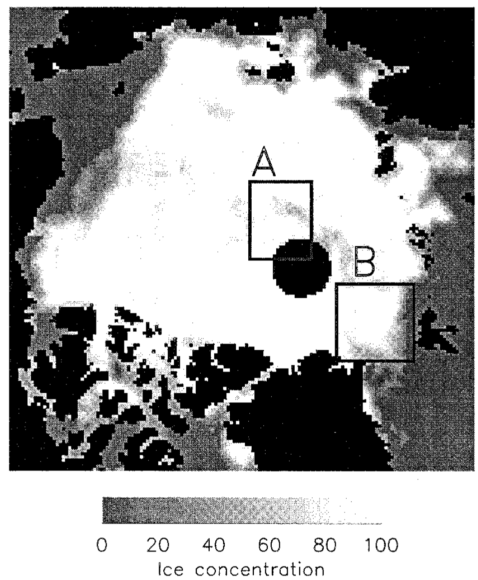

Fig. 1. September 1, 1996 Arctic ice concentration using SSM/I data and the NT2 algorithm as described in section 2. The two black boxes, labeled A and B, indicate the two regions studied in detail in this paper.

A new passive microwave sea ice concentration algorithm has recently been developed [17]. This algorithm, which is briefly described in Section II, overcomes some of the shortcomings of the original NASA Team algorithm [3]; [13] as demonstrated in Comiso *et al.* [7]. In this paper, we are investigating the behavior of the new algorithm during Arctic summer conditions. First, we take ground-based measurements of emissivities of summer sea ice conditions and analyze the resulting ice concentrations for both the NASA Team and the new algorithm (Section III). We also investigate the temporal evolution of SSM/I brightness temperatures and the retrieved sea ice concentrations (Section IV). For validation, we compare the SSM/I ice concentrations with SAR sea ice concentration retrievals during September 1996 (Section V). Fig. 1 shows the two areas investigated (black boxes). In the central Arctic (box A), the SAR data cover the period from September 1, 1996 through September 7, 1996 and for the area closer to the ice edge (box B), SAR data are available for the period September 15, 1996 through September 22, 1996. These areas are coincident with ship-borne measurements. When the cloud cover disappeared, the outgoing thermal radiation often cooled the atmosphere close to the ground forming fog. The average ice thickness varied from 8 cm to 56 cm, with a thin snow cover (8 cm to 15 cm) located at 85 °N, 10 °E and southward to the marginal ice zone. In the eastern high Arctic there were no signs that a summer melt had taken place, since relatively high salinity was found in the surface parts of the second-year ice cores, investigated along the transect 85 °N 149 °E to 160 °E. On the other hand, areas closer to the ice edge i.e., south of 85 °N along 10 cm °E had experienced melting conditions. This conclusion is based on the large number of frozen melt ponds found in this part of the Arctic. Typically, the ponds were covered by 10 to 20 cm of fresh ice above a layer of fresh water on multiyear ice. Preliminary analysis of the scan SAR wide radarsat imagery from 15 and 21 August 1996 indicates that ice concentration in the high Arctic was on average 85%, which was close to visual observations made from the icebreaker bridge.

II. SSM/I Brightness Temperatures and Ice Concentrations

The brightness temperatures (T_B) from the DMSP special sensor microwave imager (SSM/I) are daily averages mapped onto a polar-stereographic projection map (commonly referred to as the SSM/I grid) available at the National Snow and Ice Data Center, Boulder, CO [*NSIDC*, 1992]. Ice concentrations have been derived using an enhanced version of the NASA Team sea ice concentration algorithm [17] (hereafter referred to as the NT2 algorithm). Similar to the original NASA Team (NT) algorithm [3]; [5], [6] it uses ratios of brightness temperatures in order to account for variations in physical temperature, but in addition to the 19 GHz and 37 GHz channels, the enhanced algorithm utilizes also the 85 GHz channels of the SSM/I. The incentive for using the 85 GHz channels was to correct for low concentration biases caused by surface effects primarily in parts of the Antarctic. In the NT algorithm, tiepoints for open water (OW), first-year (FY) ice and multiyear (MY) ice using the polarization at 19 GHz,

$$PR(19) = \frac{T_B(19V) - T_B(19H)}{T_B(19V) + T_B(19H)} \quad (1)$$

and the spectral gradient ratio between 37 GHz and 19 GHz at vertical polarization,

$$GR(37V19V) = \frac{T_B(37V) - T_B(19V)}{T_B(37V) + T_B(19V)} \quad (2)$$

span a triangle in which the fractions for each of the three surface types and thus, ice concentrations are calculated [Fig. 2(a)]. Low ice concentration biases result primarily from the sensitivity of the 19 GHz horizontal polarization channel to inhomogeneities such as layering in the snow cover. These lead to reduced values of $T_B(19H)$ that result in higher $PR(19)$ values and thus, in lower ice concentrations. As this sensitivity is not apparent in the horizontal polarization channel at 85 GHz the ratio difference

$$\Delta GR = GR(85H19H) - GR(85V19V) \quad (3)$$

provides an estimate of the amount of layering with $T_B(19H)$ being the only channel affected. Thus, ΔGR enables the identification of an additional surface type, labeled C. With increasing layering effects ΔGR will also increase. In order to obtain ice concentrations the NT2 algorithm additionally uses the ratios $PR_R(19)$ and $PR_R(85)$. These are polarizations rotated (therefore the subscript R) through an angle, ϕ, which is the angle between the $GR(37V19V)$-axis and the FY-MY line [see Fig. 2(a)] following

$$PR_R(\nu) = -GR(37V19V) \times \sin\phi_\nu + PR(\nu) \times \cos\phi_\nu \quad (4)$$

where ν is either 19 GHz or 85 GHz. The angles ϕ_ν for 19 and 85 GHz and for both hemispheres are given in [17]. This makes the rotated polarizations independent of FY and MY ice type fractions. Because of the increasing sensitivity to atmospheric effects with increasing frequency the new algorithm applies a forward atmospheric radiative transfer model to correct for weather in the ice concentration retrievals. Therefore, we not only have one tiepoint for each surface type but several for each modeled atmospheric state. Fig. 2(b) and 2(c) show scatter plots of the same SSM/I data as in Fig. 2(a) for ΔGR versus $PR_R(19)$ and ΔGR versus $PR_R(85)$, respectively. Modeled ratios (tiepoints) for the pure surface types with different atmospheric conditions are indicated as grey circles. Fig. 3(a) presents a flow chart of the algorithm. The ratios $PR_R(19)$, $PR_R(85)$, and ΔGR are calculated from the measured SSM/I brightness temperatures (this set is labeled $\mathbf{R}$ in Fig. 3(a). We also calculate these ratios from our model data for all ice concentrations (in 1% increments) and various atmospheric conditions ($\langle\mathbf{R}\rangle$) in Fig. 3(a) and then find the best agreement between the measured and modeled ratios for each pixel. It has been demonstrated in [17] that this approach effectively corrects for cloud contamination particularly in areas of lower ice concentrations such as in the marginal sea ice zone.

VI. Conclusions

The evolution of summer time passive microwave signatures and ice concentration are investigated and the results are compared with SAR ice concentration retrievals. This analysis shows that the NT2 sea ice concentration algorithm is better than the traditional NASA Team algorithm during the summer season. The agreement of NT2 results with the SAR retrievals is very good whereas the NT algorithm underestimates ice concentration. The reason for the improvement is based on the utilization of the 85-GHz channels and the definition of an added surface type in addition to the standard first-year and multiyear ice types. This new ice type represents areas with significant amount of inhomogeneities or layering in the snow cover. These inhomogeneities are particularly common during the summer when frequent melt and freeze events alter the snow/ice structure. Nevertheless, this study only gives hints of when and why the NT2 algorithm performs better than the NT algorithm. Dedicated high-resolution passive microwave measurements with coincident in-situ measurements of the snow/ice physical and radiative properties as well as with atmospheric observations are needed to more completely evaluate the algorithm and possibly suggest further improvements.